2023 IEEE International Instrumentation and Measurement Technology Conference (I2MTC) | 978-1-6654-5383-7/23/$31.00 ©2023 IEEE | DOI: 10.1109/I2MTC53148.2023.10176060

DELiB: Deep Extreme Learning-Based Health Estimation for Lithium-ion Battery

Murukuri S V S V Vasanth
Dept of DSAI
IIIT Naya Raipur, India
murukuri20102@iiitnr.edu.in

Paul Akash Gunturu
Dept of CSE
IIIT Naya Raipur, India
paul20100@iiitnr.edu.in

Aparna Sinha
Dept. of ECE
IIIT Naya Raipur, India
aparna.sinha@ieee.org

Debanjan Das
Dept of ECE
IIIT Naya Raipur, India
debanjan@ieee.org

***Abstract*—The accurate estimation of the State of Health (SoH) and Remaining Useful Life (RUL) of Lithium-ion batteries are of great significance for the safety and performance of electric vehicles (EVs). However, the existing SoH estimation techniques involve non-dynamic feature extraction without considering time and computation cost, leading to challenges in real-time implementation on batteries with varying specifications. To address these issues, this paper proposes a novel hybrid model, *DELiB*, designed by integrating Convolution neural networks (CNN) and Extreme Learning Machines (ELM) to estimate SoH and RUL of the batteries. The proposed model automatically extracts highly correlated features to the target and performs the predictions within a short period. *DELiB* was tested on four batteries with different specifications from two publicly available datasets. The model accurately estimates the SoH and RUL with an average root mean squared error (RMSE) of 0.0021 and 0.023, respectively, in 0.5 ms. Moreover, the result proves the robustness of the *DELiB* model under varying charge-discharge profiles and temperature profiles. The model can quickly estimate the SoH and RUL using low-end computational resources, which proves its suitability for real-time EV applications.**

***Index Terms*—EVs, Lithium-ion battery, SoH, RUL, CNN, ELM.**

I. Introduction

The usage of Electric Vehicles (EVs) has exponentially increased in the past ten years. The safety and reliability of EVs are largely dependent on battery health. The most popular and often used EV batteries are Lithium-ion Batteries [1]. They have higher energy and power level, lesser self-discharge, and long lifeline. Despite many advantages, Li-ion batteries' performance deteriorates with time due to unavoidable internal chemical reactions and external conditions, such as aging and overcharging [2]. The unexpected fault may result in emergent maintenance and catastrophic event such as fire explosions. Hence, it is crucial to accurately estimate the lithium-ion battery's health to ensure the whole system's safety.

In Battery Health Management (BHM), [3] State of Health (SoH) and Remaining Useful Life (RUL) are essential parameters in determining the condition of the system. SoH of a battery is the ratio of present capacitance to the initial capacitance. The RUL gives the idea of how many cycles the battery will function without fail or the cycles remaining to reach the end of life (EOL).

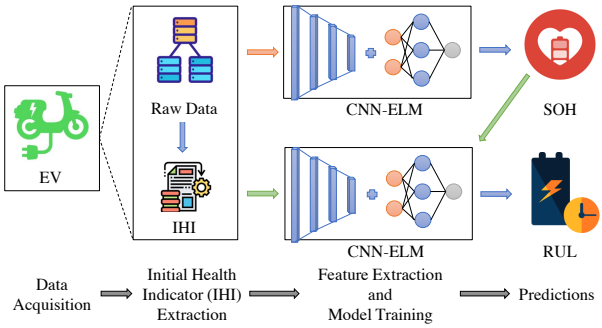

Fig. 1. Overview of the proposed solution

In this regard, various approaches have emerged for the health prognosis of Li-ion batteries, including (i) electrochemical-based, (ii) empirical-based, and (iii) data-driven-based methods. The first two methods are difficult to implement in real-time. Moreover, the empirical methods are sensitive to changes in operating conditions and battery parameter variations. In this endeavor, data-driven methods have gained popularity in recent times because of the quick progress in fields like the Internet of Things (IoT), Artificial Intelligence (AI), Machine Learning (ML), and Deep Learning (DL).They are non-parametric and do not need any knowledge of internal systems beforehand [4]. For the health prognosis of Lithium-ion batteries, many data-driven approaches are proposed [5] [6]. One of the major challenges of battery health prediction is to extract the right and optimized features to be fed into the SoH and RUL prediction model. Most existing works extract the features manually, leading to error accumulation and increased extraction time [4].

With this motivation, a hybrid DL-based solution, *DELiB*, has been devised, which can automatically extract beneficial features from any battery and perform the SoH and RUL prediction quickly and accurately. From the accumulated data, initial health indicators are extracted and fed to the hybrid model. Further, the model automatically extracts positively correlated features and predicts the SoH and RUL of the battery Fig. 1 provides a synopsis of the conceptual framework of our solution. The Novel Contributions are:

- An algorithm was proposed for the extraction of opti-

mized initial health indicators from raw data to reduce the time and complexity of the proposed DL model. This approach reduces the data nearly 700 times the original, making it computationally efficient.

- A hybrid CNN-ELM model has been proposed that extracts the highly correlated features and accurately predicts the battery SoH and RUL. The incorporation of ELM makes the model lightweight and capable of faster learning and generalized performance.
- The proposed model has experimented on four distinct batteries. The predictions yielded an average RMSE of 0.00287 for SoH and 0.025 for RUL.
- The effects of temperature and different charge-discharge profiles were studied and evaluated based on the case studies to ensure the robustness and practical applicability of the proposed hybrid model.

II. Related Works and Research Gaps

TABLE I
REVIEW OF THE EXISTING SOLUTIONS

Paper	Method	Dataset	MSD	SoH & RUL	Evaluation Metrics
[5]	GPR, SVM, MGPR	NASA	×	×	MAE: 0.12 - 0.98
[7]	RVM	CALCE	×	✓	MAE: 0.0081 - 0.012
[6]	SA-LSTM	NASA	×	×	MAE: 0.0250
[8]	DEKF	HPPC	×	✓	–
[9]	LSTM with Attention	eVTOL	✓	×	RMSE: 0.0027
[10]	SVR, GPR & ELM	Dynamic Experiment	×	✓	–
DELiB	**CNN-ELM**	**eVTOL; CALCE**	✓	✓	**RMSE: 0.0021, MAE: 0.0017**

MSD: Multi-source dataset

The new age of modern EVs is increasing and will further be the future of modern society. It's high time to monitor and prioritize the health indicators of the batteries. The estimation of SoH and RUL of lithium-ion batteries need to be improved for safety and to avoid catastrophic events. Much research is going on in this field, and there are three widely-used approaches: Model-based, data-driven, and hybrid. Model-based approaches need dissecting the battery, the knowledge of electrochemistry, and vast knowledge of circuits and chemical substances.

In [8], the estimation of SoC and SoH is carried out using Dual Extended Kalman Filter (DEKF) method; there are dual filters where the initial filter is used for the calculation of the State of Charge and the second filter passes the health of battery parameters. The estimation of SoC and SoH is improved, but the filter method requires experimental subjects to analyze the life cycle, considering the battery capacity and charging reduction behavior. Fan *et al.* [7] developed a battery prediction method that uses a Gaussian filter that relies on IC (Internal-Charge) curve using the Relevance Vector Machine method.

Data-driven methods use the previous data of the battery and extract the hidden information, which is helpful for SoH and RUL estimation of the battery. Zheng *et al.* [5] proposed an SoH estimation through the MGPR process model. The health indicators (HIs) are selected using mutual information analysis. This gives a great result, but the performance degrades for different types of batteries with different conditions, and the feature needs to be manually extracted. Many Statistical models are implemented along with Deep learning methods. The non-parametric regression technique that the SVR algorithm suggests can be updated by model retraining. In order to predict RUL and create a prediction model based on SVR, Patil *et al.* [10] used the feature vectors collected from the voltage and temperature curve as the input data set. The model's RMSE is 0.357%. Upper and lower errors when the confidence interval is 95% are 7.87% and 10.75%, respectively. In order to increase the SVR's accuracy, During the charging and discharging operation, the voltage difference can be varied at various time intervals, Zhao *et al.* [10] estimated the battery capacitance. The method of processing the data set when the feature vector is selected was then integrated with this calculation. Yang *et al.* [6] implemented SA-LSTM, which fit well in the network of real values. The features are extracted automatically with good accuracy, and the health indicators are well extracted using a neural network with the time series method. But the computational time is the drawback that is necessary if the Battery Health Monitoring System needs to be checked regularly. The summary of the comparative analysis of *DELiB* with prior works is represented in Table I.

III. Proposed Methodology

A. Dataset Description

1) eVTOL Dataset: This dataset comprises 124 commercial Li-ion phosphate (LFP)/graphite cells, which were fast-charged in a temperature chamber at 30°C. The cells' nominal voltage is 3.3 V, and their nominal capacity is 1.1 Ah [11]. The dataset is broken into three "batches", approximately 48 cells each. The "batch date", or the day the tests began, identifies each batch.

2) CALCE Dataset: All the batteries in this dataset were charged according to the same methodology. The constant current charging phase (CC) and the constant voltage charging phase are both included in the charging protocol (CV). Every charging cycle was run until the voltage matched the charging cutoff voltage at a charge rate of 0.5 C (0.55 A) (4.2 V). Once the current exceeded the predetermined cutoff current, the voltage was kept at the cutoff voltage (0.05 A and 1C) [12]. Information on the batteries utilized in this paper is provided in Table II.

TABLE II
SPECIFICATIONS OF THE LI-ION BATTERIES

Dataset	S.no	Battery-ID	Charge Profile	T°C
eVTOL	B1	el150800737368	5C(67%)-4C	30°C
	B2	el150800737285	5.9C(60%)-3.1C	
CALCE	B3	CS2-35	CCCV,0.5C	24°C
	B4	CS2-37	CCCV,0.5C	

B. Initial Health Indicator Extraction

For calculating the actual SoH from the capacitance measured at each cycle, Eq 1 is used, where C_{pres} represents present battery capacitance, and C_{init} represents initial battery capacitance or the capacitance of the battery when manufactured.

$$SoH = \frac{C_{pres}}{C_{init}}. \tag{1}$$

Even though CNN can extract valuable features from the raw data. But the enormous data size makes it difficult for the model to train and extract the features resulting in high time and computational complexities. Hence extracting the initial health indicators (IHIs) mean and rate of change per cycle can be a better solution to make the model computationally efficient and less complex. For Current and Voltage, we prefer mean as they are predetermined inputs to the battery, and for the rest, we compute the rate of change as they depend on the battery's performance. Algorithm-1 provides a better understanding of the initial health indicators extraction.

Algorithm 1 : *IHI extraction*

Input: 1. $Features(f_1, f_2, ...f_k)$ {Raw features of a cycle}
1: Computing IHIs for a cycle
2: **for** x = 1 to k **do**
3: **if** f_i is $Current(\mathbf{I})or Voltage(\mathbf{V})$ **then**
4: Calculate feature mean using the equation: $f_{xm} = \sum_{y=1}^{n} \frac{f_{xy}}{n}$
5: **else**
6: Calculate the feature rate using the equation : $f_{xr} = \frac{f_x(max) - f_x(min)}{CycleDuration}$
7: **end if**
8: **end for**
Output: Initial health indicators

C. SoH and RUL Prediction

The IHI's were next passed to Convolution Neural Network (CNN) to extract new features that benefit the prediction.

1) CNN-Feature Extraction: CNN mainly consists of 2 layers Convolution and Pooling. In the convolutional layer, the input data is convolved with various kernels resulting in feature maps. Convolution consistently preserves spatial data and creates numerous maps. The pooling layer's function is to reduce the size of the feature map by spatial-invariance average (Average Pooling) or maximum operation (Max Pooling). The Convolution and the pooling layers work to extract useful features from the input data. In this paper, we use 1D Convolution as the data was single-dimensioned. Compared to 2D Convolution, 1D Convolution requires less computational power as it requires a smaller number of layers for extracting helpful insights compared to 2D Convolution [13].

Let x be a vector of length K multiplied or convolved with a vector filterω which is of length M. This operation is known as Convolution. Convolution has been expressed in Eq.2 and produces a one-dimensional layer a of length $(K - M + 1)$.

$$\boldsymbol{a}(n) = g\left(\sum_{i=0}^{M-1} \omega(i)\boldsymbol{x}(n-i) + b\right), \quad n = 0, 1, \ldots, K-1, \tag{2}$$

In Eq. 2, b represents bias, and $g(x)$ is an activation function which is a non-linear function. The activation function used in this paper is Rectified Linear Unit (*ReLU*). In this proposed CNN structure, after four convolutions, the produced feature map is pooled by using the Maxpooling operation, in which the highest possible value of k in a kernel window function, where the stride is s and size $n * 1$, k takes the vector a as the input and produce an output vector m. This operation is defined in Eq. 3:

$$m = max(k(n * 1, s), a). \tag{3}$$

We have four convolution layers for feature extraction. For designing the architecture, we started with one convolution layer and kept on increasing the convolution layers until the desired results were obtained. After pooling, the data was flattened. This flattened data is further processed using Artificial Neural Networks (ANN), resulting in five new features that act as input for the ELM.

2) ELM-Prediction: Extreme Learning Machines (ELMs) contain single feed-forward neural networks (SLFNs), capable of learning faster than traditional approaches like gradient-based techniques. It is a typical neural network with one hidden layer but no learning process. ELM does not undergo iterative tuning; instead, the hidden nodes are initialized randomly and fixed. The only parameters which need tuning are the weights between the output layer and hidden layers. As ELM does not undergo iterative tuning, it works faster and gives a generalized performance compared to the networks which use back-propagation [4].

Let δ denotes the connections between hidden and input layers, b is the hidden layer's bias, and α represents the weight of the output. The input is given as $I = (\mathbf{x}_i, a_i)|\mathbf{x}_i = (x_{i1}, ..., x_{in})^T \epsilon A^n, a_i = (a_{i1}, ..., a_{in})^T \epsilon A^m$, where $\mathbf{x}_i$ is the input value and a_i is the target value. Then, the ELM model which has $\hat{P}$ hidden neurons produces an output **o** is computed by the Eq 4

$$\sum_{k=1}^{\hat{K}} \alpha_k f(\delta_k \mathbf{x}_j + b_k) = \mathbf{o}_n, n = 1, 2, ..., K, \tag{4}$$

where $f(x)$ represents the hidden layer's activation function and *ReLU* is the activation function used in the ELM model. The Eq. 4 can be computed using the Eq 5:

$$\mathbf{W}\beta = \mathbf{Z}, \tag{5}$$

where $\mathbf{W}$ and $\mathbf{Z}$ are the matrices of hidden and output layers, respectively. Therefore, utilizing Eq. 5, the weights between output and hidden layers can be processed by the Eq 6

$$\beta = \mathbf{W}^{\dagger}\mathbf{Z}. \tag{6}$$

where $\mathbf{W}^{\dagger}$ represents the Moore–Penrose generalized inverse of the matrix $\mathbf{W}$. Fig. 2 gives an idea of the hybrid model's architecture. We use the same architecture for the RUL Prognosis, but along with the pre-processed features, SoH acts as an input to the hybrid model (CNN-ELM) for the estimation of RUL.

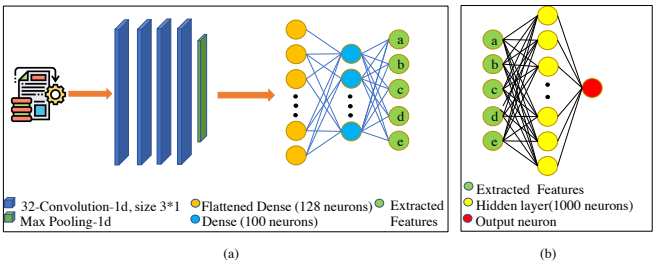

Fig. 2. The Hybrid CNN-ELM Model Architecture (a) Feature Extraction (b) Prediction using the extracted features

IV. Results And Discussion

Using Algorithm 1, the IHIs were extracted from the raw data. It has reduced the data by 700 times the initial, making the model less complex and computationally efficient. The hybrid model uses the extracted IHIs to estimate SoH and RUL.

A. SoH & RUL Prediction Results

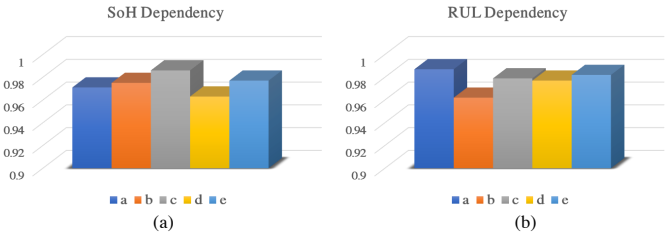

Fig. 3. Bar plots depicting the dependencies of (a) SoH and (b) RUL on extracted features.

1) SoH estimation: The proposed hybrid model predicts the SoH of four batteries from Table II. Features extracted by CNN cannot be used directly for the estimation; verifying the target's dependency on the extracted features is essential. Their dependency is evaluated using the Pearson correlation coefficient. Let a_j is the j^{th} predictor of the k predictors, and b_j is the j^{th} target of the k targets. Therefore, the correlation coefficient is computed using the equation 7.

$$c = \frac{\Sigma_{j=1}^{k}(a_j - \bar{a})(b_j - \bar{b})}{\sqrt{\Sigma_{j=1}^{n}(a_j - \bar{a})^2 \Sigma_{j=1}^{k}(b_j - \bar{b})^2}}, \tag{7}$$

where $\bar{a}$ is

$$\bar{a} = \frac{1}{k}\Sigma_{j=1}^{k} a_j \tag{8}$$

and $\bar{b}$ is

$$\bar{b} = \frac{1}{k}\Sigma_{j=1}^{k} b_j \tag{9}$$

From Fig. 3, we can observe the high dependency of the extracted features. The predicted results are evaluated using Root Mean Squared Error (RMSE) and Mean Absolute Error (MAE). These can be computed using the Eq. 10-11. The values of the metrics (RMSE, MAE) are inversely proportional to the model's accuracy, which implies that if the metrics are minimal, the model is accurate. The evaluated metrics of four batteries were given in Table III.

$$\text{RMSE} = \sqrt{\frac{\sum_{i=1}^{n}(\text{SoH}_{\text{actual}_i} - \text{SoH}_{\text{predicted}_i})^2}{n}}, \tag{10}$$

$$\text{MAE} = \frac{|\text{SoH}_{\text{actual}} - \text{SoH}_{\text{predicted}}|}{n}, \tag{11}$$

The model was trained with three types of splits: (1) Initial 60% for training, (2) Initial70% for training (3) Initial 80% for training. The model was trained using these three types of splits and tested on the left data to show the dependability and effectiveness of the model and to demonstrate that the model can work effectively even with fewer data. The predicted results are shown in Fig. 4. The metrics and the results represent that the proposed architecture can accurately estimate SoH, and the model's performance increases with the data given for training.

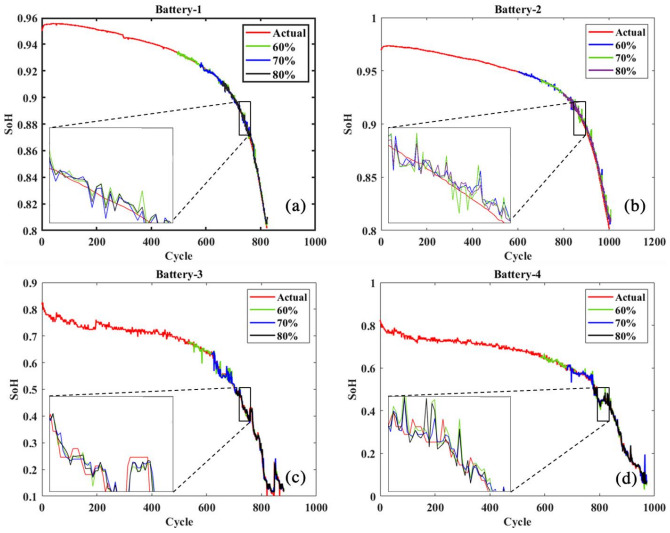

Fig. 4. SoH Predictions of (a) B1 (b) B2 (c) B3 (d) B4.

2) RUL estimation: The same *DELiB* architecture is used for the RUL prediction, but the only difference is that along with the other features, SoH will also become an input for the prediction of RUL. The dependencies of the extracted features are represented in Fig. 3. For a better understanding, instead of RMSE and MAE, we evaluate the RUL prediction results using Absolute Error. The absolute error (AE) can be

TABLE III
EVALUATION OF SOH PREDICTIONS

S.no	RMSE Test	RMSE Valid	MAE Test	MAE Valid	Duration(s)
B1	0.0021	0.0025	0.0014	0.0022	0.068
B2	0.0026	0.0028	0.0017	0.0024	0.073
B3	0.0033	0.0037	0.0025	0.0017	0.069
B4	0.0035	0.0042	0.0027	0.0026	0.071

computed using the Eq. 12, where $|x|$ and $[x]$ are modulus and step functions, respectively. The model was trained by taking the initial 80% of the data. Similar to RMSE and MAE, the value of AE should be lower to justify the model's performance. The errors produced by the model while predicting RUL for the four chosen batteries are shown in Table IV. Fig. 5 represents how accurate were the predictions made by the model on the four batteries.

$$\text{AE} = [|RUL_{actual} - RUL_{predicted}|]. \tag{12}$$

TABLE IV
EVALUATION OF RUL PREDICTIONS

S.no	RUL Actual	RUL Predicted	AE
B1	824 cycles	820 cycles	5 cycles
B2	1002 cycles	994 cycles	8 cycles
B3	882 cycles	878 cycles	4 cycles
B4	972 cycles	965 cycles	7 cycles

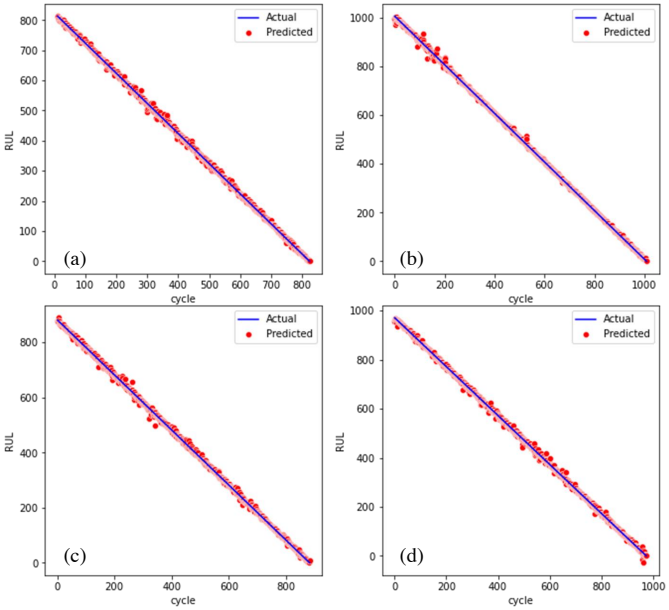

Fig. 5. RUL Predictions of (a) B1 (b) B2 (c) B3 (d) B4.

3) Computational complexity: Our experimental setup has 8GB RAM, an Intel i5 processor, a 64-bit system, and a Windows 11 operating system. Under this setup, the trained model estimated the target at 0.5 ms.

B. Verification of model's robustness

1) Evaluation of the model's performance with different charge and discharge profiles: This case study checks the model's effectiveness on batteries with different charge-discharge profiles. We tested our model on B1 (*eVTOL*) and B3 (*CALCE*). The profiles of the batteries were mentioned in Table II. Fig. 6 shows the detailed results of B1 and B3's SoH estimation. The RMSE of the predictions for B1 is 0.0021 and B3 is 0.0035, and the AE is less than 0.008. The results have shown that the model is accurate, robust and can estimate SoH irrespective of the charge-discharge profile.

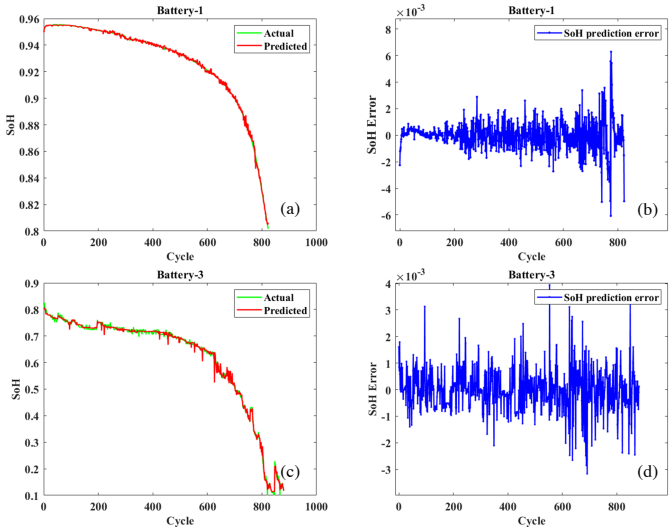

Fig. 6. (a) & (c) SoH prediction of B1 & B3, (b) & (d) SoH prediction error of B1 & B3, under different charge-discharge profiles.

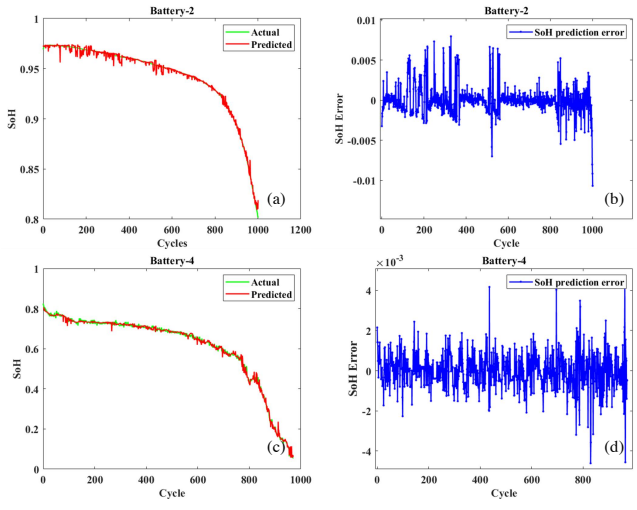

Fig. 7. (a) & (c) SoH prediction of B2 & B4, (b) & (d) SoH prediction error of B2 & B4, under different temperatures.

2) Evaluation of the model's performance at various temperatures: This case study verifies the model's working ability at different functioning temperatures. We tested our model on B2 (*eVTOL*) and B4 (*CALCE*). From the Table II,

the functioning temperatures of B2 (30°C) and B4 (24°C) are different. Fig. 7 depicts the detailed results of SoH estimation. The results have demonstrated that the model can precisely estimate SoH irrespective of operating temperature conditions. The RMSE of the predictions of B2 is 0.0025, B4 is 0.0033, and the AE is less than 0.01.

3) Observations and Hypothesis:

- The results of the studies show a considerable increment in the error value for the last 200 cycles compared to the initial cycles.
- When a battery hits its end of life (EOL; SOH = 0.8 to 0.7), the degradation rate accelerates exponentially, rendering it unusable.
- , Therefore, this relatively significant error is acceptable, considering that no operational data exists beyond EOL.

C. Comparative Analysis

The SOTA models taken into account in this study are the GPR (statistical algorithm), SVM (machine learning), and LSTM (Deep learning). Table-V, Table-VI compare the effectiveness of SoH and RUL predictions using various SOTA methods. Compared to the other models, the CNN-ELM model provided the lowest RMSE.

TABLE V
COMPARATIVE ANALYSIS OF SOH PREDICTIONS

Model	RMSE Test	MAE Test	RMSE Valid	MAE Valid
CNN-ELM	**0.0021**	**0.0017**	**0.0032**	**0.0022**
GPR	0.0058	0.0038	0.0081	0.0043
LSTM	0.029	0.024	0.032	0.0082
SVM	0.0132	0.0074	0.032	0.0082

TABLE VI
COMPARATIVE ANALYSIS OF RUL PREDICTIONS

Model	RMSE Test	MAE Test	RMSE Valid	MAE Valid
CNN-ELM	**0.0234**	**0.0142**	**0.0243**	**0.0162**
GPR	0.3216	0.2925	0.4565	0.4396
LSTM	0.0743	0.0526	0.725	0.0483
SVM	0.0132	0.0174	0.032	0.0082

V. CONCLUSION AND FUTURE WORK

Using manually extracted or existing health indicators to estimate the State of Health (SoH) and Remaining Useful Life (RUL) may be inadequate in real-world scenarios due to the unpredictable and random nature of real-time data. The accuracy and dependencies of these models can differ from battery to battery based on their specifications, and the training process is lengthy and complex, making the models cumbersome. A new Hybrid Model is developed to overcome the above-mentioned problems. The paper's main conclusions are (1) Extraction of IHIs, reducing complexity, and making the model computationally efficient. (2) The IHIs were fed to the hybrid model that automatically extracts the valuable features and estimates SoH and RUL. (3) The model has given 0.00287 average RMSE and 0.0017 average MAE; the same approach estimates the battery's RUL. The hybrid model produced 0.023 average RMSE and 0.0142 average MAE. (4) The suggested method was tested on batteries with different charge-discharge and temperature profiles to demonstrate robustness. The future work includes validation of our model with other battery datasets to verify its robustness and generality. We can further integrate Explainable Artificial Intelligence (XAI) to bring the trustworthiness of the used deep learning model to the users.

REFERENCES

[1] R. Thomas, G. Despesse, S. Bacquet, E. Fernandez, Y. Lopez, P. Ramahefa-Andry, and L. Cassarino, "A high frequency self-reconfigurable battery for arbitrary waveform generation," *World Electric Vehicle Journal*, vol. 12, no. 1, p. 8, 2021.

[2] X. Hu, Y. Che, X. Lin, and S. Onori, "Battery health prediction using fusion-based feature selection and machine learning," *IEEE Trans. Transport. Electrific.*, vol. 7, no. 2, pp. 382–398, 2020.

[3] A. Marisetty, P. R. Medi, A. Sinha, and D. Das, "DaSoR: Data-driven State-of-Health & Remaining Useful Life Estimation of Li-ion Batteries in a Closed-loop system of Electric Vehicles," in *2022 IEEE Delhi Section Conference (DELCON)*. IEEE, 2022, pp. 1–5.

[4] A. Sinha, D. Das, V. Udutalapally, and S. P. Mohanty, "iThing: Designing Next-Generation Things With Battery Health Self-Monitoring Capabilities for Sustainable IIoT," *IEEE Trans. Instrum. Meas.*, vol. 71, p. 3528409, 2022.

[5] X. Zheng and X. Deng, "State-of-health prediction for lithium-ion batteries with multiple Gaussian process regression model," *IEEE Access*, vol. 7, pp. 150 383–150 394, 2019.

[6] Y. Ge, F. Zhang, and Y. Ren, "Lithium ion battery health prediction via variable mode decomposition and deep learning network with self-attention mechanism," in *Frontiers in Energy Research*, 2022.

[7] Y. Fan, J. Qiu, S. Wang, X. Yang, D. Liu, and C. Fernandez, "Incremental Capacity Curve Health-Indicator Extraction Based on Gaussian Filter and Improved Relevance Vector Machine for Lithium–Ion Battery Remaining Useful Life Estimation," *Metals*, vol. 12, no. 8, p. 1331, 2022.

[8] A. Wang, H. Chen, P. Jin, J. Huang, D. Feng, and M. Zheng, "RUL Estimation of Lithium-Ion Power Battery Based on DEKF Algorithm," in *2019 14th IEEE Conference on Industrial Electronics and Applications (ICIEA)*. IEEE, 2019, pp. 1851–1856.

[9] T. Mamo and F.-K. Wang, "Attention-based long short-term memory recurrent neural network for capacity degradation of lithium-ion batteries," *Batteries*, vol. 7, no. 4, 2021. [Online]. Available: https://www.mdpi.com/2313-0105/7/4/66

[10] S. Jin, X. Sui, X. Huang, S. Wang, R. Teodorescu, and D.-I. Stroe, "Overview of machine learning methods for lithium-ion battery remaining useful lifetime prediction," *Electronics*, vol. 10, no. 24, 2021. [Online]. Available: https://www.mdpi.com/2079-9292/10/24/3126

[11] F.-K. Wang, Z. E. Amogne, C. Tseng, and J.-H. Chou, "A hybrid method for online cycle life prediction of lithium-ion batteries," *International Journal of Energy Research*, vol. 46, no. 7, pp. 9080–9096, 2022.

[12] W. He, N. Williard, M. Osterman, and M. Pecht, "Prognostics of lithium-ion batteries based on dempster–shafer theory and the bayesian monte carlo method," *Journal of Power Sources*, vol. 196, no. 23, pp. 10 314–10 321, 2011.

[13] I. Mitiche, A. Nesbitt, S. Conner, P. Boreham, and G. Morison, "1D-CNN based real-time fault detection system for power asset diagnostics," *IET Generation, Transmission & Distribution*, vol. 14, no. 24, pp. 5766–5773, 2020.